10-19-2004

In situ transmission electron microscopy study of the electric field-induced transformation of incommensurate modulations in a Sn-modified lead zirconate titanate ceramic

H. He
Iowa State University

Xiaoli Tan
Iowa State University, xtan@iastate.edu

In situ transmission electron microscopy study of the electric field-induced transformation of incommensurate modulations in a Sn-modified lead zirconate titanate ceramic

Abstract
Electric field-induced transformation of incommensurate modulations in a Sn-modified lead zirconate titanate ceramic was investigated with an electric field*in situ*transmission electron microscopy technique. It is found that the spacing between the (1/x){110}satellite spots and the fundamental reflections do not change with external electric field, indicating that the modulation wavelength stays constant under applied field. The intensity of these satellites starts to decrease when the field level reaches a critical value. Further increase in the field strength eventually leads to the complete disappearance of the satellite reflections. In addition, the 12{111}-type superlattice reflections showed no response to electrical stimuli.

Keywords
Transmission electron microscopy, Electric fields, Stellites, Ferroelectric phase transitions, Phase transitions, Ozone, Antiferroelectric phase transitions, Antiferroelectricity, Lead, Ceramics

Disciplines
Ceramic Materials | Materials Science and Engineering

Comments
The following article is from *Applied Physics Letters* 85 (2004): 3187 and may be found at http://dx.doi.org/10.1063/1.1805179.

In situ transmission electron microscopy study of the electric field-induced transformation of incommensurate modulations in a Sn-modified lead zirconate titanate ceramic

H. He and X. Tan

Citation: Applied Physics Letters **85**, 3187 (2004); doi: 10.1063/1.1805179
View online: http://dx.doi.org/10.1063/1.1805179
View Table of Contents: http://scitation.aip.org/content/aip/journal/apl/85/15?ver=pdfcov
Published by the AIP Publishing

In situ transmission electron microscopy study of the electric field-induced transformation of incommensurate modulations in a Sn-modified lead zirconate titanate ceramic

H. He and X. Tan[a)]
Department of Materials Science and Engineering, Iowa State University, Ames, Iowa 50011

(Received 7 May 2004; accepted 11 August 2004)

Electric field-induced transformation of incommensurate modulations in a Sn-modified lead zirconate titanate ceramic was investigated with an electric field *in situ* transmission electron microscopy technique. It is found that the spacing between the $(1/x)\{110\}$ satellite spots and the fundamental reflections do not change with external electric field, indicating that the modulation wavelength stays constant under applied field. The intensity of these satellites starts to decrease when the field level reaches a critical value. Further increase in the field strength eventually leads to the complete disappearance of the satellite reflections. In addition, the $\frac{1}{2}\{111\}$-type superlattice reflections showed no response to electrical stimuli. © *2004 American Institute of Physics*. [DOI: 10.1063/1.1805179]

Incommensurate modulations have been observed experimentally with transmission election microscopy (TEM) in many perovskite ferroelectric ceramics, such as $PbZrO_3$,[1] $Pb(Zr_{1-x}Ti_x)O_3$,[2,3] Sn-modified $Pb(Zr_{1-x}Ti_x)O_3$ (PZST),[4–7] La-modified $Pb(Zr_{1-x}Ti_x)O_3$ (PLZT),[8–10] $Pb(Co_{1/2}W_{1/2})O_3$,[11,12] and $Pb(Sc_{1/2}Ta_{1/2})O_3$.[12,13] They are characterized by the satellite reflections in electron diffraction patterns and the regular fringes in image contrast. The modulation wave vector represented by the satellites is along the normal direction of those fringes, and the distance of the satellites to the fundamental reflections in reciprocal space corresponds to the spacing of the fringes in real space. The wave vector is parallel to the $\langle 110\rangle$ direction in most cases and the wavelength lies in the range of $5\sim 20a$, where a is the lattice parameter for the parent paraelectric structure.[8]

Transformation of the intermediate incommensurate phase to other phases can be triggered by external stimuli, such as chemical composition and temperature.[6–10] Sn- or Ti-content in the PZST system and La content in the PLZT system were utilized before as controlling variables for the phase transformation.[8–10] In the PZST system, it has been shown that decrease in Sn content or increase in Ti content leads to the incommensurate antiferroelectric-to-ferroelectric phase transformation. In the PLZT system, the modulation wavelength was observed to increase with Ti molar fraction.[8] Utilizing temperature as the controlled variable in the study of such transformations allows *in situ* TEM studies, where the evolution of the satellite reflections can be directly observed.[6,7] The hot-stage *in situ* TEM observations revealed that the modulation wavelength increases continuously with increasing temperature. Based on these studies, Viehland *et al.*[8] suggested that the competing ferroelectric and antiferroelectric ordering in these perovskites are responsible for the presence of incommensurate modulations. However, unambiguous evidence has yet to be found. In this letter, we report the study of the incommensurate phase transformation triggered by controlled electric fields. The evolution of the satellite spots driven by external electrical stimuli is recorded.

A hybrid coprecipitation method similar to that used by Yang and Payne[14] was followed to prepare the ceramic powder with a chemical formula $Pb_{0.99}Nb_{0.02}[(Zr_{0.55}Sn_{0.45})_{0.94}Ti_{0.06}]_{0.98}O_3$ (abbreviated as PZST 45/6/2). Pressed cylinders, 15 mm in diameter by 20 mm thick, were formed by cold-isostatic pressing at 350 MPa. The preformed pellets were then hot pressed in an Al_2O_3 die at 1150 °C for 2 h in air. Thin slices from the hot-pressed piece were annealed at 1300 °C for 2 h in an atmosphere containing excess PbO. The annealed slices were then ground, polished, and electroded. Dielectric characterization was performed with an LCR meter (HP-4284A, Hewlett-Packard) at frequency of 1 kHz in conjunction with an environmental chamber. A heating rate of 3 °C/min was used during measurement. Electric field-induced polarizations were recorded with a standardized ferroelectric test system (RT-66A, Radiant technologies).

TEM specimens were prepared from ultrasonically cut 3-mm-diam disks. The thickness of these disks was reduced to ~150 μm by grinding and polishing. The center portion was further thinned to ~10 μm by dimpling. The dimpled specimens were then annealed at 300 °C for 30 min to minimize residual stresses. An argon ion mill was used for further thinning until final perforation occurred in the center. Gold electrodes with spacing of 250 μm were evaporated to the TEM specimens, and platinum wires were used to connect the electrodes to the electrical contacts on the TEM specimen holder. Figure 1 shows the schematic diagram of the TEM specimen configuration. Details of the electric field *in situ* TEM technique can be found elsewhere.[15–18] TEM studies were carried out on a Phillips CM-30 microscope operating at 300 kV.

Temperature dependence of the dielectric permittivity of PZST 45/6/2 is shown in Fig. 2. The dielectric constant peaks with a value of 920 at the temperature of 167 °C. Electric field-induced polarization measurement showed double hysteresis loops (Fig. 3), indicating an electric field-induced antiferroelectric-to-ferroelectric phase transformation at room temperature. These results are consistent with previous observations from other researchers.[5–7]

In order to determine the field level needed for the *in situ*

[a)]Electronic mail: xtan@iastate.edu

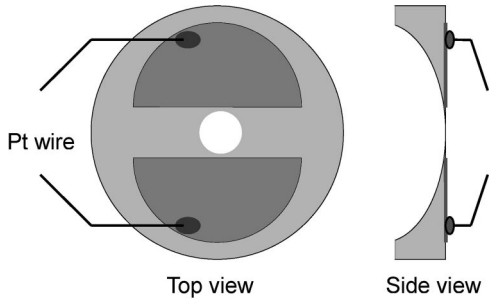

FIG. 1. Schematic diagram of specimens for the electric field *in situ* TEM study.

TEM study and to assess the sample geometry effect on the field-induced antiferroelectric-to-ferroelectric phase transformation, a dimpled and annealed 3-mm-diam disk specimen was tested for the hysteresis measurement and the result is also plotted in Fig. 3. Compared to the conventional circular plate sample with electric field applied along the thickness direction, the TEM-specimen-like disk shows a more gradual phase transformation with much broader loops. Furthermore, the backward switch from the induced ferroelectric phase to the antiferroelectric phase is sluggish, and a nonzero remnant polarization is detected.

In situ TEM studies were carried out on a disk specimen with a central perforation. Actual electric field in the specimen is disturbed (intensified in some areas while diluted in others) by the presence of the perforation. Electron transparent areas that are subjected to intensified electric fields in the specimen were located in the TEM and one grain within this area was focused for the successive detailed *in situ* study. For an ideal circular perforation, the intensification ratio is 2.[19] The local electric field strength in this grain was thus estimated by doubling the nominal field strength.

The evolution of the satellite spots in a ⟨112⟩-zone axis selected area diffraction pattern under static electric fields is shown in Fig. 4. Initially, this grain displays one set of incommensurate modulations. In the electron diffraction pattern, one set of the $(1/x)\{110\}$ satellite spots is evident, as shown in Fig. 4(a). No detectable changes to these satellite spots were observed with applied static electric field up to 40 kV/cm. At the field level of 48 kV/cm, these satellites become weaker in their intensity [Fig. 4(b)]. This field level lies in the close vicinity of the E_F (the critical field to trigger the antiferroelectric-to-ferroelectric transformation) measured from the bulk sample. However, careful measurement indicates that the modulation wavelength does not change with increasing field strength. When the field strength reached 56 kV/cm, most satellite spots disappeared. As shown in Fig. 4(c), only very weak satellites can be barely seen surrounding the three strong fundamental reflections in the left of this micrograph. The field strength was then reduced to 40 kV/cm. The satellites reappeared, with the strongest ones sitting in the upper-left corner of Fig. 4(d). When the field level was raised again to 56 kV/cm [Fig. 4(e)], all the satellite spots completely disappeared, indicating the complete transformation to the ferroelectric phase. After the electric field was completely removed, no satellite spots were observed to reappear, as shown in Fig. 4(f). The observation confirms the sluggish nature of the backward ferroelectric-to-antiferroelectric transformation that has been noticed by other researchers in a similar composition.[20]

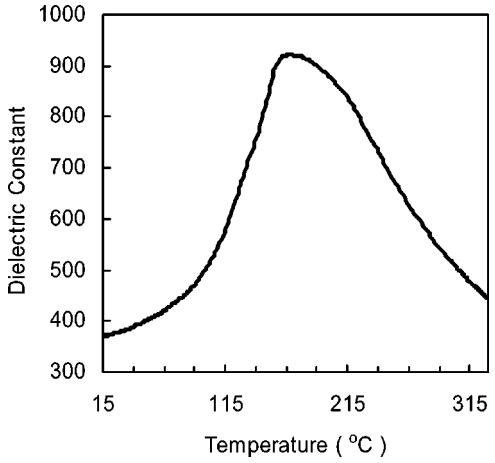

FIG. 2. Temperature dependence of dielectric constant at 1 kHz in the PZST 45/6/2 ceramic.

It has been suggested that in PZT-based ferroelectric perovskites, the presence of incommensurate modulations in the antiferroelectric phase is a result of the competition between the ferroelectric and antiferroelectric ordering.[8] The continuous increase in the modulation wavelength with increasing temperature is interpreted that there exists a ferroelectric phase within a narrow temperature range just below the paraelectric transition temperature. When temperature is raised close to this temperature range the ferroelectric ordering is enhanced. The modulation wavelength is thus increased. However, our observations on the electric field-induced transformation of the incommensurate modulation show a different scenario. The intensity of the satellite reflections, rather than the modulation wavelength, changes with the applied electric field strength. The wavelength stays constant at a value of 2.3 nm. Since external electric field is known to enhance the ferroelectric ordering, we suggest that the electric field-induced antiferroelectric (incommensurate)-to-ferroelectric transformation proceeds as following. When the applied electric field reaches E_F, the phase transformation is initiated in some areas of the grain. The transformation is an abrupt one and no intermediate changes in the modulation wavelength takes place. With increasing electric field strength, the fraction of the transformed area increases and the intensity of the satellite diffraction peaks gets weaker.

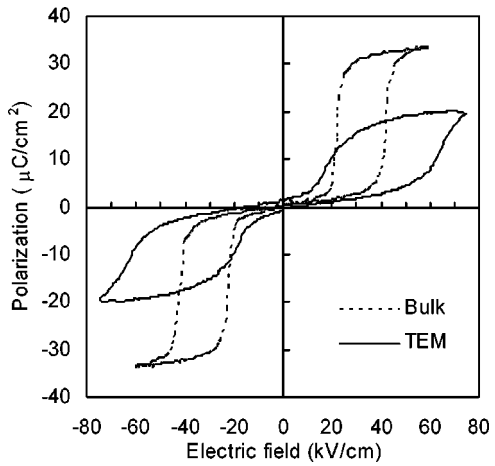

FIG. 3. Electric field-induced polarization measurement at 4 Hz in a bulk circular plate sample and an unperforated TEM specimen.

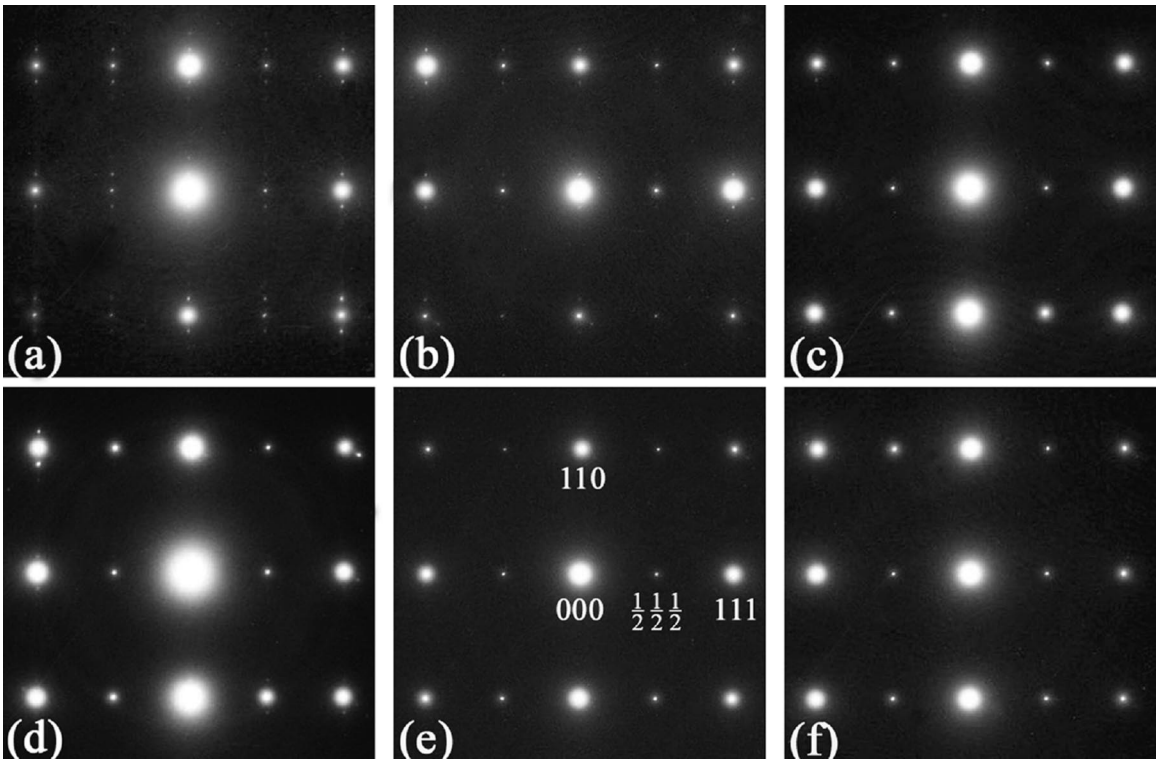

FIG. 4. Evolution of the ⟨112⟩ selected area diffraction pattern under applied electric fields in PZST 45/6/2. (a) Original state, (b) 48, (c) 56, (d) 40, and (e) 56 kV/cm, and (f) field removed.

Obviously, a mechanism involving the nucleation of ferroelectric phase and the motion of the phase boundary controls the transformation process. Further studies will be focused on these issues.

In addition to the $(1/x)\{110\}$ satellite spots, $\frac{1}{2}\{111\}$-type superlattice reflections were also present in the ⟨112⟩-axis diffraction pattern, as labeled in Fig. 4(e). The structural origin for these superlattice reflections is still under debate.[2,5–7,9,21] However, the present *in situ* TEM study provides valuable insight into the physics mechanism for the presence of these superlattice reflections. It is clear in Fig. 4 that the intensity of the $\frac{1}{2}\{111\}$ spots does not change with the applied electric field, implying a mechanism that is quite rigid to external disturbance. This seems to favor the oxygen octohedra tilting model.[21]

To summarize, *in situ* TEM technique was applied to the study of the electric field-induced antiferroelectric-to-ferroelectric phase transformation in a PZT-based ceramic. Upon application of external electric fields, the wavelength of the incommensurate modulation in the antiferroelectric phase showed no change but the intensity of the satellite reflections decreased when the field exceeds a critical value. This critical strength matches closely to the E_F measured in the bulk sample.

This work was supported by the Process Science Initiative (PSI) program at Ames Laboratory, U.S. DOE (Grant No. 10-501-115612). The authors are grateful to Dr. David Cann for the access to the dielectric characterization instrument in his group at Iowa State University.

[1]Z. Xu, X. Dai, D. Viehland, and D. A. Payne, J. Am. Ceram. Soc. **78**, 2220 (1995).
[2]J. Ricote, D. L. Corker, R. W. Whatmore, S. A. Impey, A. M. Glazer, J. Dec, and K. Roleder, J. Phys.: Condens. Matter **10**, 1767 (1998).
[3]S. Watanabe and Y. Koyama, Phys. Rev. B **66**, 134102 (2002).
[4]J. S. Speck, M. De Graef, A. P. Wilkinson, A. K. Cheetham, and D. R. Clarke, J. Appl. Phys. **73**, 7261 (1993).
[5]D. Viehland, D. Forst, Z. Xu, and J. Li, J. Am. Ceram. Soc. **78**, 2101 (1995).
[6]Z. Xu, D. Viehland, P. Yang, and D. A. Payne, J. Appl. Phys. **74**, 3406 (1993).
[7]Z. Xu, D. Viehland, and D. A. Payne, J. Mater. Res. **10**, 453 (1995).
[8]D. Viehland, X. Dai, J. Li, and Z. Xu, J. Appl. Phys. **84**, 458 (1998).
[9]J. Knudsen, D. I. Woodward, and I. Reaney, J. Mater. Res. **18**, 262 (2003).
[10]Z. Xu, X. Dai, and D. Viehland, Phys. Rev. B **51**, 6261 (1995).
[11]S. Watanabe and Y. Koyama, Phys. Rev. B **65**, 064108 (2002).
[12]C. A. Randall, S. A. Markgraf, A. S. Bhalla, and K. Baba-Kishi, Phys. Rev. B **40**, 413 (1989).
[13]K. Z. Baba-Kishi and D. J. Barber, J. Appl. Crystallogr. **23**, 43 (1990).
[14]P. Yang and D. A. Payne, J. Appl. Phys. **71**, 1361 (1992).
[15]Z. Xu, X. Tan, P. Han, and J. K. Shang, Appl. Phys. Lett. **76**, 3732 (2000).
[16]X. Tan, Z. Xu, J. K. Shang, and P. Han, Appl. Phys. Lett. **77**, 1529 (2000).
[17]X. Tan, Z. Xu, and J. K. Shang, Mater. Sci. Eng., A **314**, 157 (2001).
[18]X. Tan, and J. K. Shang, Philos. Mag. A **82**, 1463 (2002).
[19]R. M. McMeeking, ZAMP **40**, 615 (1989).
[20]W. Chan, H. Chen, and E. V. Colla, Appl. Phys. Lett. **82**, 2314 (2003).
[21]D. Viehland, Z. Xu, and D. A. Payne, J. Appl. Phys. **74**, 7454 (1993).